

Supplemental Information

Peripheral Cannabinoid-1 Receptor Inverse Agonism Reduces Obesity by Reversing Leptin Resistance

Joseph Tam, Resat Cinar, Jie Liu, Gregorz Godlewski, Daniel Wesley, Tony Jourdan, Gergő Szanda, Bani Mukhopadhyay, Lee Chedester, Jieih-San Liow, Robert B. Innis, Kejun Cheng, Kenner C. Rice, Jeffrey R. Deschamps, Robert J. Chorvat, John F. McElroy, and George Kunos

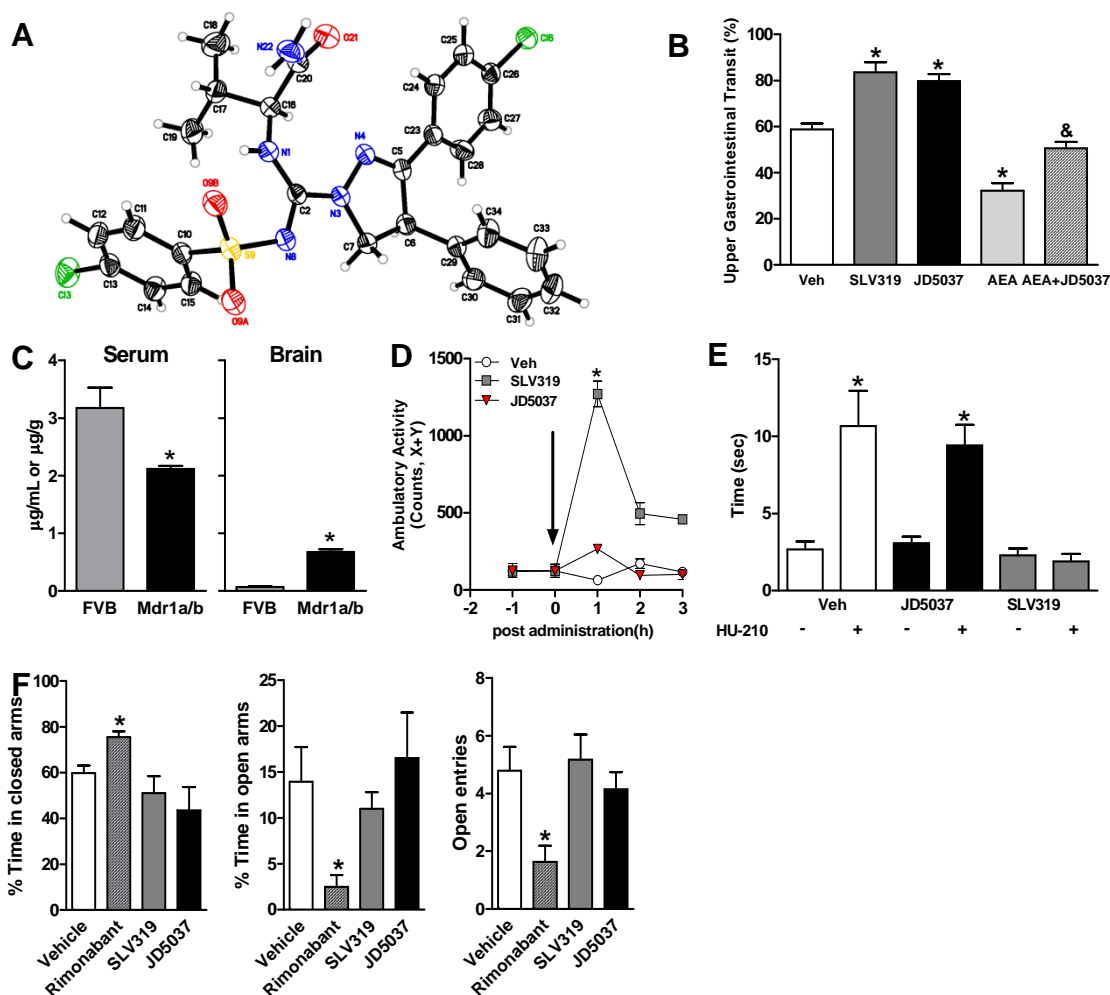
Inventory of Supplemental Information

The following supplemental table and figures provide additional information supporting the characterization of the peripheral selectivity of JD5037:

Table S1 - provides the list of 70 receptors, transporters and ion channels which have been tested and found to have at least 1,000-fold lower affinity for JD5037 relative to CB1R.

1. Figure S1 – describes the crystallographic structure of JD5037, its pharmacokinetics and behavioral profile.
2. Figure S2 – illustrates the lack of effect of JD5037 on daily and cumulative food intake and body weight of lean wild-type and CB1R KO mice
3. Figure S3 - illustrates the lack of acute effect of JD5037 on food intake, relative to SLV319, using a fasting/refeeding paradigm.
4. Figure S4 – illustrates the effects of JD5037 on energy metabolism, determined by indirect calorimetry, which complement its other metabolic effects shown in Figure 2.
5. Figure S5 – shows the effect of JD5037 on body weight and leptin sensitivity in area postrema-ablated DIO mice, ruling out this circumventricular organ as a site of action of JD5037
6. Figure S6 – illustrates the effects of JD5037 on plasma leptin and body weight in mice with chemical sympathetic denervation of the epididymal fat pads.
7. Figure S7 - illustrates the parallel effects peripheral CB1 blockade on megalin expression in the choroid plexus and on CSF:plasma ratios of leptin.

Figure S1



(A) Structure of JD5037 as determined by x-ray crystallography.

Displacement ellipsoids displayed at the 25% level; H-atoms are displayed as small circles of a fixed radius. The absolute configuration (i.e. C6 S, C16 S) was determined unambiguously from the results of the x-ray experiment and is in agreement with the known configuration of C16 which is derived from an L-amino acid used in the synthesis. The crystal structure of JD5037 has been deposited at the Cambridge Crystallographic Data Centre and allocated the deposition number CCDC 891288

(B) Effect of CB₁R agonist or antagonists on propulsive activity in mouse small intestine.

Note that both JD5037 and SLV319 (3 mg/kg, each) increased GI transit, and that JD5037 fully inhibited the decrease in GI transit caused by a maximally effective dose of anandamide (AEA, 10 mg/kg). Results are mean ± SEM of 5 mice in each group. **P*<0.05 vs. vehicle; & *P*<0.05 vs. AEA.

(C) Serum and brain levels of JD5037 in P-gp knockout mice and their wild-type controls.

Brain and plasma concentrations of JD5037 in *mdr1a/b*^{-/-} mice and their wild-type (FVB) controls 1 h after oral administration of 3 mg/kg of JD5037. Note the increase in brain levels of JD5037 in the knockout relative to wild-type mice. Data are mean ± SEM from 3 mice/group. **P*<0.05 relative to FVB.

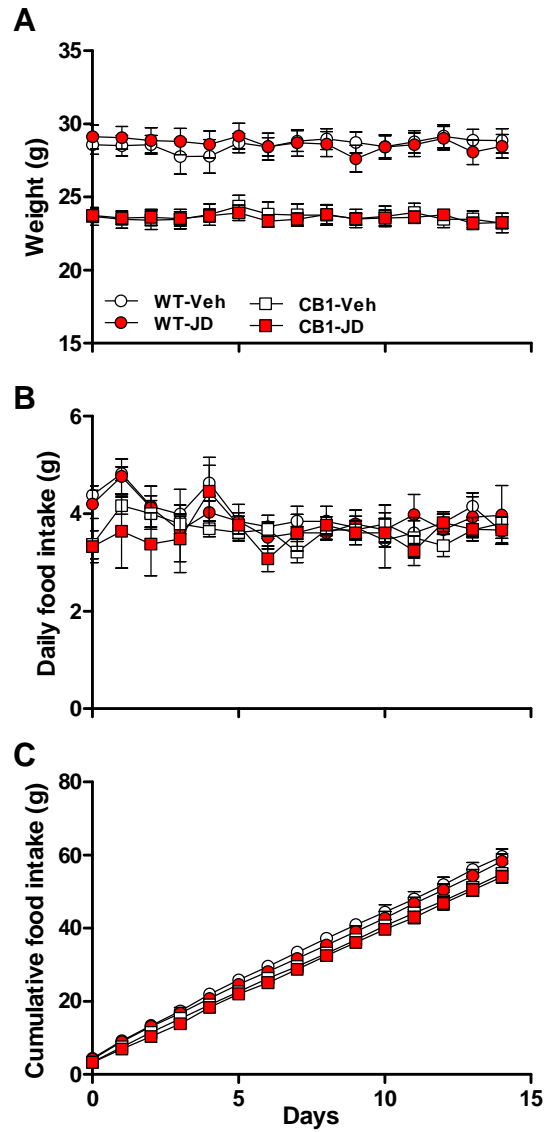
(D-F) Behavioral activity profile of JD5037 and SLV319.

(D) SLV319, but not JD5037, increases ambulatory activity. Disruption of infrared xy beams in control mice treated with vehicle or drugs (3 mg/kg, po). Arrow marks time of drug administration. Data represent mean ± SEM from 4 mice per group. **P*<0.01 relative to corresponding vehicle value.

(E) SLV319, but not JD5037, inhibits HU-210-induced catalepsy, as measured by the bar assay. The antagonists (3 mg/kg po) were given 15 min prior to the ip. injection of 30 µg/kg HU-210. Data represent mean ± SEM from 5 mice/group. **P*<0.01 relative to corresponding value in the absence of HU-210.

(F) Acute treatment with rimonabant, but not JD5037 or SLV319 (each at 3 mg/kg po), has anxiogenic effect in the elevated plus maze. Data represent mean ± SEM from 6-7 mice/group. **P*<0.05 relative to vehicle.

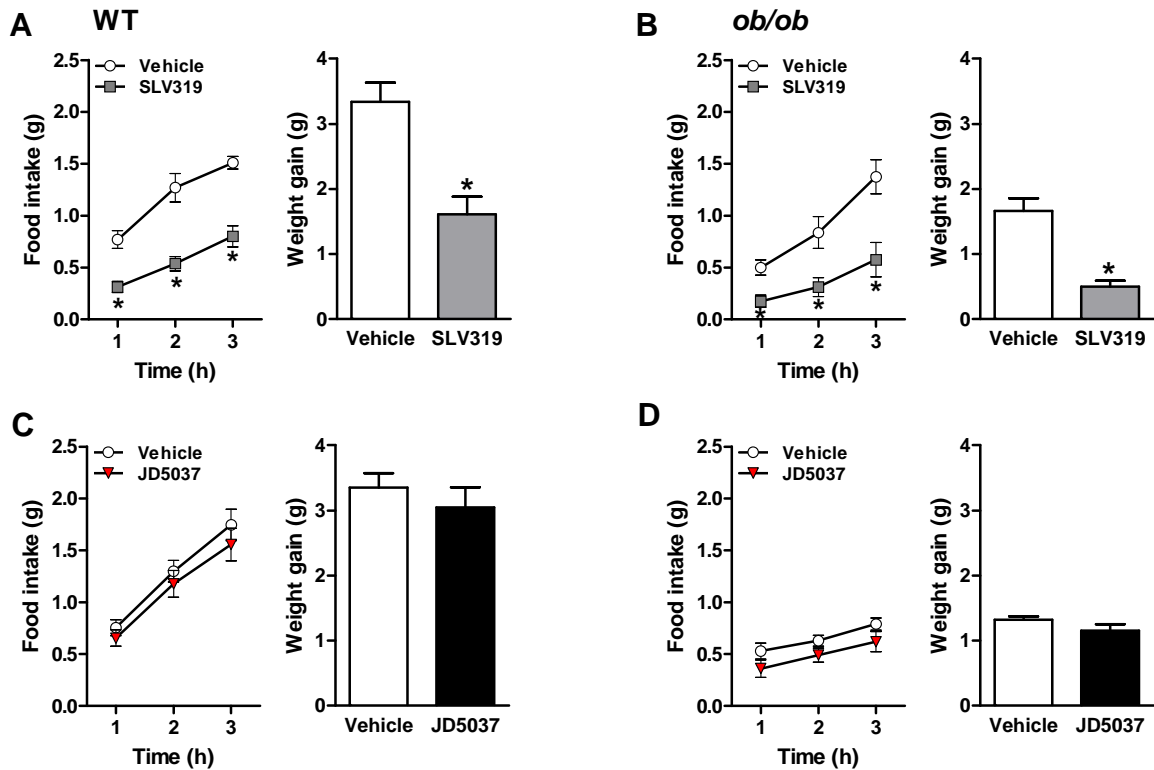
Figure S2



Effect of JD5037 on body weight and food intake in wild-type and $CB_1R^{-/-}$ mice on standard diet

Wild-type (WT) and $CB_1R^{-/-}$ mice fed STD were treated with JD5037 (3 mg/kg/day) or vehicle for 14 days, and body weight (A), daily food intake (B) and cumulative food intake (C) were monitored daily. Data are mean \pm SEM from 5 mice per condition. Note the lack of effect of JD5037 in lean control and $CB_1R^{-/-}$ mice.

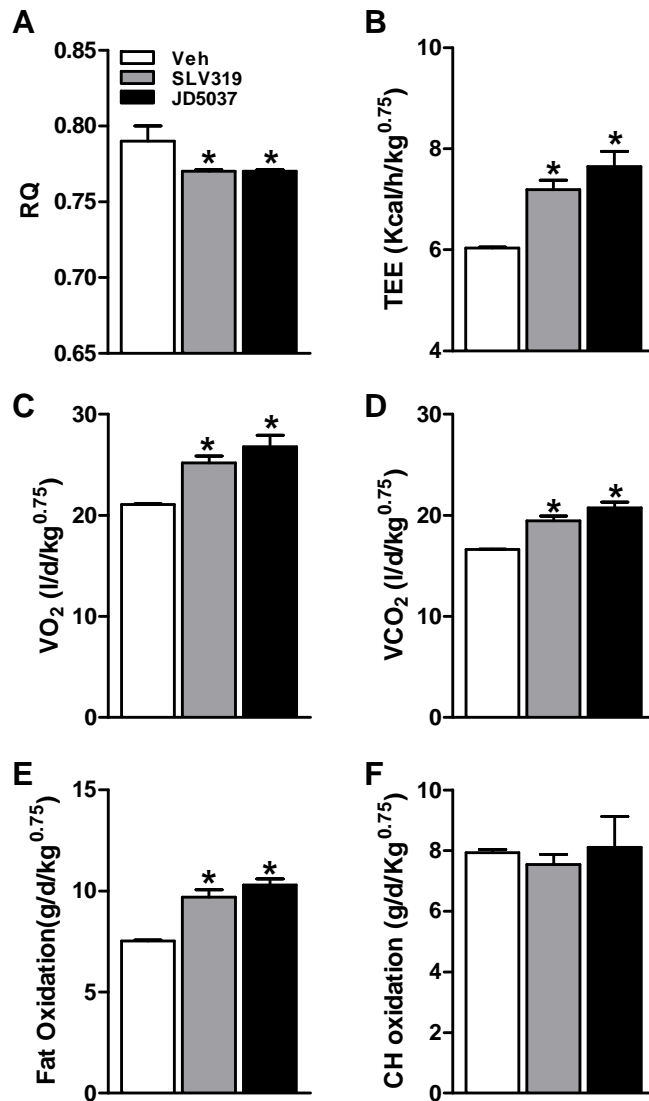
Figure S3



Acute effect of JD5037 and SLV319 on food intake and body weight gain in mice, using fasting/refeeding paradigm.

Food intake and body weight gain were measured in fasted wild-type (A, C), and *ob/ob* (B, D) mice after acute oral treatment with vehicle (white), JD5037 (black/red) or SLV319 (gray) (each at 3 mg/kg). Note that SLV319, but not JD5037, inhibited food intake (left panels) and body weight gain (right panels) in wild-type and *ob/ob* mice, suggesting that the acute effect of CB₁ blockade on food intake is centrally mediate and leptin-independent. Mice were fasted for 24 h and then injected with the drugs 30 min before the test period. Body weight gain was measured 12 h post drug administration. Data represent mean ± SEM from 4-10 animals in each group (* p<0.05).

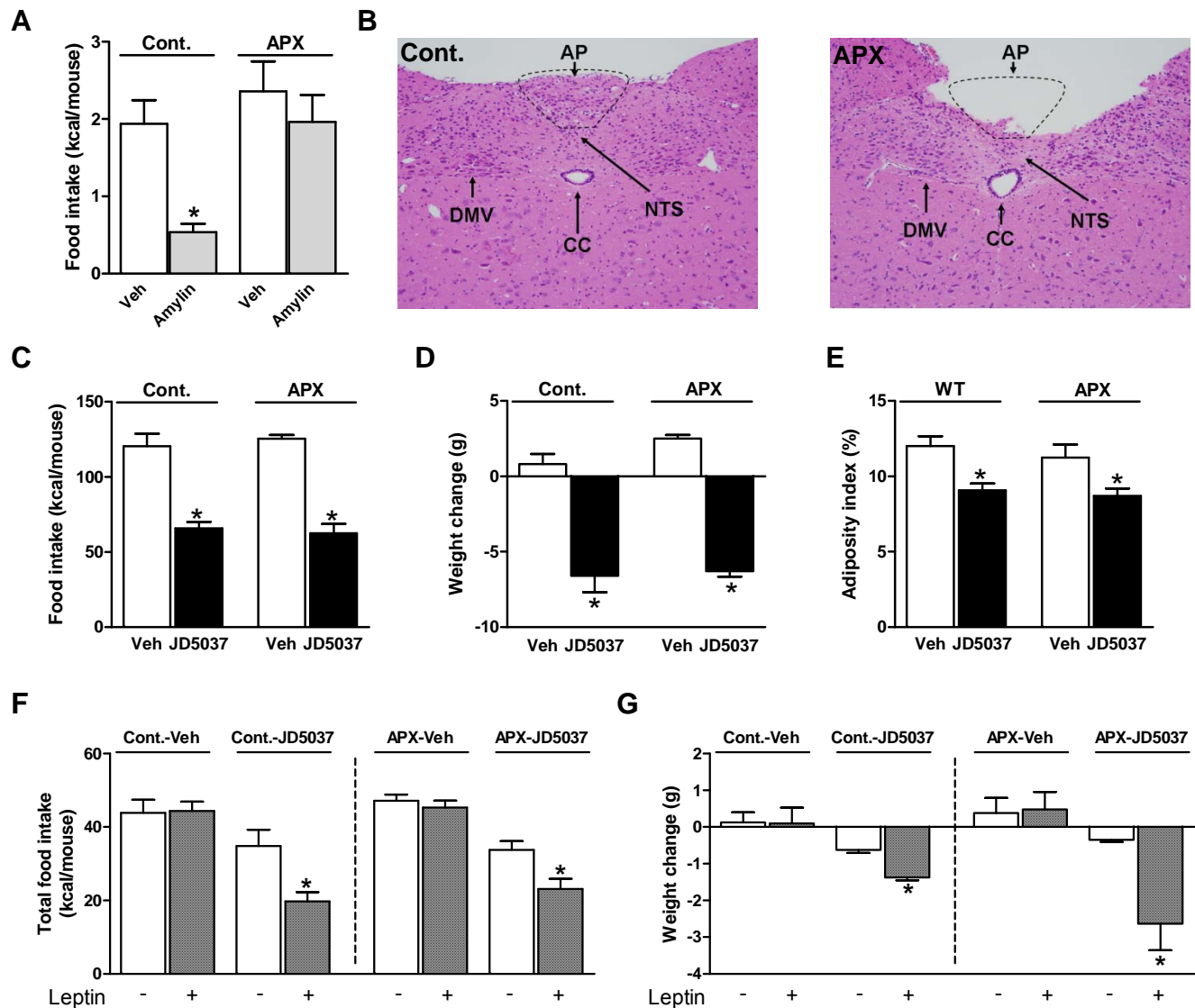
Figure S4



Effect of chronic treatment with JD5037 or SLV319 on metabolic parameters.

Daily treatment of DIO mice with JD5037 or SLV319 (each at 3 mg/kg po) for 21 days induces changes in RQ (A), total energy expenditure (B), VO₂ (C), VCO₂ (D), fat oxidation (E), but no change in carbohydrate oxidation (F), as measured by indirect calorimetry over a 24 h period at the end of the treatment. Data are mean ± SEM from 3-4 mice per condition. *P < 0.05 relative to values in vehicle-treated DIO mice .

Figure S5



The area postrema (AP) is not involved in mediating the anorexic/weight reducing effect of JD5037 .

(A) Acute effect of amylin (5 µg/kg, ip) on food intake in 24 h food-deprived area postrema-ablated (APX) and control DIO mice. Note the loss of the anorectic response in the APX mice

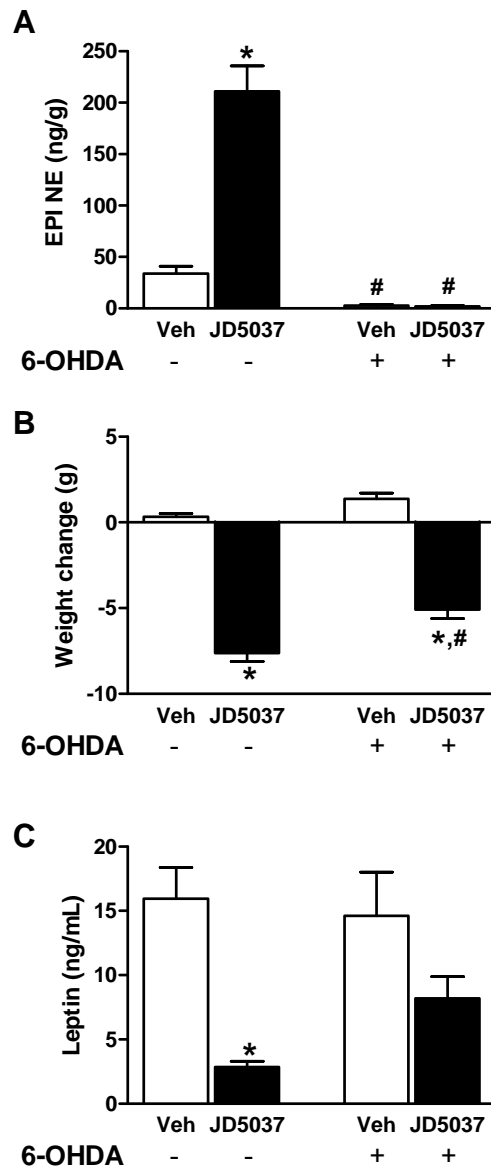
(B) Representative photomicrograph of histological sections through the AP region from one APX and control mice. Tissue was stained with hematoxylin eosin.

(C-E) Effects of 7-day treatment with JD5037 (3 mg/kg, po) on cumulative food intake (C), weight (D) and adiposity (E) are similar in APX and control DIO mice.

(F-G) Effects of leptin (3 mg/kg twice daily for 4 days) on food intake (F) and weight (G) are similar in APX and control DIO mice treated for 7 days with JD5037, 3 mg/kg/day po.

Data are mean ± SEM from 6 mice /group. * P<0.05 relative to corresponding vehicle-treated group.

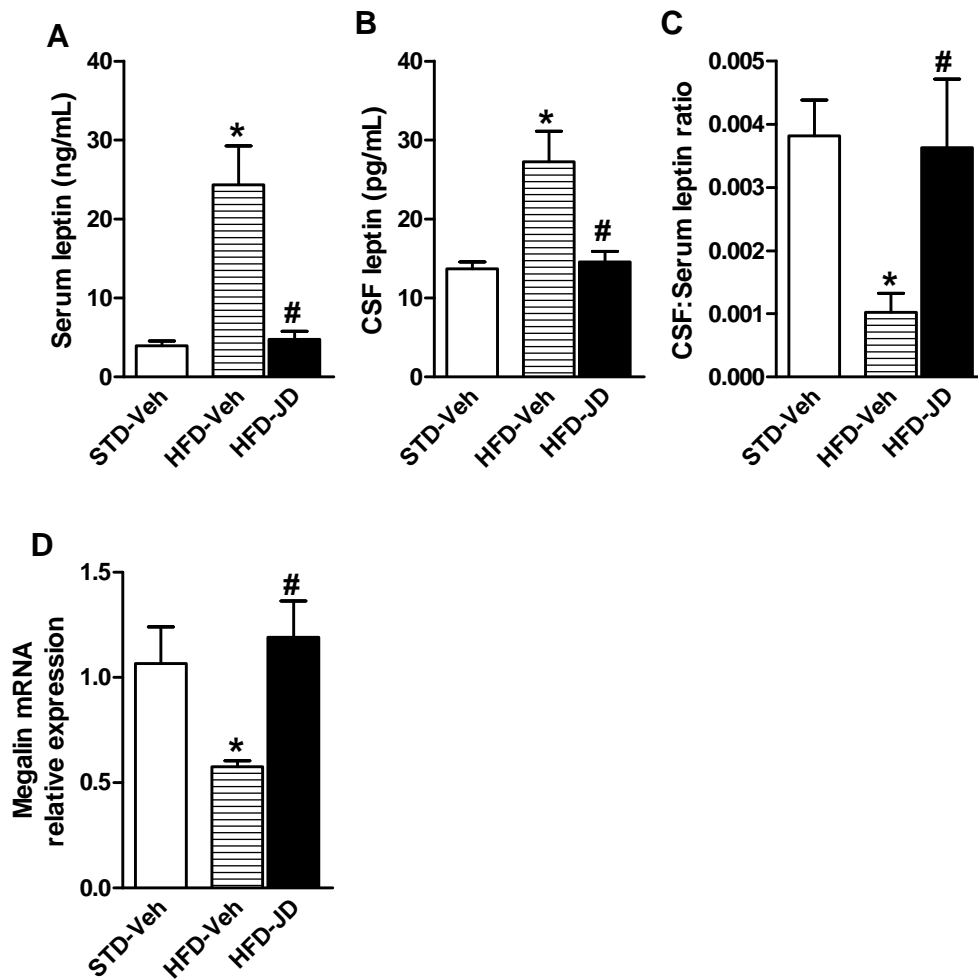
Figure S6



Effect of JD5037 on serum leptin in DIO mice with chemical sympathetic denervation of the epididymal fat pad.

Norepinephrine (NE) content of epididymal fat pad (EPI) (A), body weight change (B) and serum leptin levels (C) were measured in control DIO mice or in DIO mice with 6-OHDA-induced denervation of EPI. Mice were treated with vehicle (white) or JD5037 (3 mg/kg/day, po) for 1 week (black). 6-hydroxydopamine (6-OHDA; 10 mg/ml) or vehicle were injected into the EPI of DIO mice. After 2-week recovery, the animals were treated orally with either JD5037 or vehicle. Note that (1) the NE content of 6-OHDA-injected EPI pads is drastically reduced and is unaffected by JD5037 treatment, and (2) the efficacy of JD5037 in reducing body weight and serum leptin levels is attenuated in the 6-OHDA-treated mice. Data are mean \pm SEM from 5 mice per condition. * $P < 0.05$ relative to the corresponding vehicle group, # $P < 0.05$ relative to either vehicle or JD5037 treated animals in the control group.

Figure S7



Effect of JD5037 on serum and cerebrospinal fluid (CSF) leptin levels (A-C) and on megalin mRNA in choroid plexus.

Compared to STD-fed mice, HFD-fed mice have higher serum (A) and CSF leptin levels (B), but lower CSF:serum leptin ratio (C) and lower megalin expression in the choroid plexus (D). 7-day treatment of HFD-fed mice with JD5037 (3 mg/kg, po) normalizes all these parameters. Data are mean \pm SEM from 5-6 mice per condition. *P<0.05 relative to STD-vehicle group, # P<0.01 relative to HFD-vehicle group.

Table S1

A_1 (<i>h</i>) (antagonist radioligand)	NK_1 (<i>h</i>) (agonist radioligand)
A_{2A} (<i>h</i>) (agonist radioligand)	NK_2 (<i>h</i>) (agonist radioligand)
A_3 (<i>h</i>) (agonist radioligand)	NK_3 (<i>h</i>) (antagonist radioligand)
α_1 (non-selective) (antagonist radioligand)	Y (non-selective) (agonist radioligand)
α_2 (non-selective) (antagonist radioligand)	N neuronal $\alpha_4\beta_2$ (<i>h</i>) (agonist radioligand)
β_1 (<i>h</i>) (agonist radioligand)	opioid (non-selective) (antagonist radioligand)
β_2 (<i>h</i>) (agonist radioligand)	NOP (ORL_1) (<i>h</i>) (agonist radioligand)
AT_1 (<i>h</i>) (antagonist radioligand)	$PPAR_\gamma$ (<i>h</i>) (agonist radioligand)
AT_2 (<i>h</i>) (agonist radioligand)	PCP (antagonist radioligand)
BZD (central) (agonist radioligand)	EP_2 (<i>h</i>) (agonist radioligand)
B_1 (<i>h</i>) (agonist radioligand)	IP (PGI_2) (<i>h</i>) (agonist radioligand)
B_2 (<i>h</i>) (agonist radioligand)	$P2X$ (agonist radioligand)
CB_1 (<i>h</i>) (agonist radioligand)	$P2Y$ (agonist radioligand)
CB_2 (<i>h</i>) (agonist radioligand)	$5-HT$ (non-selective) (agonist radioligand)
CCK_1 (CCK_A) (<i>h</i>) (agonist radioligand)	σ (non-selective) (agonist radioligand)
CCK_2 (CCK_B) (<i>h</i>) (agonist radioligand)	GR (<i>h</i>) (agonist radioligand)
CRF_1 (<i>h</i>) (agonist radioligand)	ER (non-selective) (<i>h</i>) (agonist radioligand)
D_1 (<i>h</i>) (antagonist radioligand)	PR (<i>h</i>) (agonist radioligand)
D_{2S} (<i>h</i>) (antagonist radioligand)	AR (<i>h</i>) (agonist radioligand)
D_3 (<i>h</i>) (antagonist radioligand)	TRH_1 (<i>h</i>) (agonist radioligand)
$D_{4,4}$ (<i>h</i>) (antagonist radioligand)	V_{1a} (<i>h</i>) (agonist radioligand)
ET_A (<i>h</i>) (agonist radioligand)	V_2 (<i>h</i>) (agonist radioligand)
ET_B (<i>h</i>) (agonist radioligand)	Ca^{2+} channel (L, dihydropyridine site) (antagonist radioligand)
$GABA$ (non-selective) (agonist radioligand)	Ca^{2+} channel (L, diltiazem site) (benzothiazepines)(antagonist radioligand)
$AMPA$ (agonist radioligand)	Ca^{2+} channel (L, verapamil site) (phenylalkylamine)(antagonist radioligand)
ketate (agonist radioligand)	K_{ATP} channel (antagonist radioligand)
$NMDA$ (antagonist radioligand)	ζ_v channel (antagonist radioligand)
H_1 (<i>h</i>) (antagonist radioligand)	SK_{Ca} channel (antagonist radioligand)
H_2 (<i>h</i>) (antagonist radioligand)	Cl^- channel (GABA-gated) (antagonist radioligand)
H_3 (<i>h</i>) (agonist radioligand)	norepinephrine transporter (<i>h</i>) (antagonist radioligand)
I_1 (agonist radioligand)	dopamine transporter (<i>h</i>) (antagonist radioligand)
I_2 (antagonist radioligand)	$GABA$ transporter (antagonist radioligand)
BLT_1 ($-TB_4$) (<i>h</i>) (agonist radioligand)	choline transporter (CHT1) (<i>h</i>) (antagonist radioligand)
$CysLT_1$ (LTD_2) (<i>h</i>) (agonist radioligand)	$5-HT$ transporter (<i>h</i>) (antagonist radioligand)
MC_4 (<i>h</i>) (agonist radioligand)	M (non-selective) (antagonist radioligand)
MT_1 (ML_A) (<i>h</i>) (agonist radioligand)	

JD5037 is greater than 1,000x selective for CB1 over a 70 receptor/ion channel panel (Diversity Profile by Cerep, Celle l'Evescault, France).

At a concentration of 1 μ M, JD5037 caused <50% suppression in radioligand binding assays for the targets listed above.

SUPPLEMENTAL EXPERIMENTAL PROCEDURES

Synthetic procedures and compound characterization

The precursors for the synthesis of JD5037 have previously been described (Lange et al., 2004). The pyrazoline 2 was made in two steps from a phenylacetophenone via a Mannich reaction and subsequent condensation with hydrazine (Scheme 4 in alange et al., 2004). Subsequent conversion of the pyrazoline to the amino ester adduct was carried out by the steps shown in Scheme 5 with L-valine methyl ester used instead of methylamine. The ester was hydrolyzed using LiOH in aqueous THF solution, and the resulting acid was coupled with ammonia/THF in dichloromethane solution in the presence isobutyl chloroformate and N-methylmorpholine at room temperature to afford the amino-carboxamide adduct as a mixture of diastereomers. Flash chromatography (silica gel, pet ether/ethyl acetate) followed by recrystallization (dichloromethane/pet ether) produced the high affinity diastereomer, JD5037. NMR (CD₃OD): 1.04, 6H, d; 4.15, 1H, brd s; 4.5, 1H, brd s; 4.67 1H, brd s; 4.89, 1H, brd s; 7.48, 2H, d; 7.66, 2H, d; 7.87, 2H, d. MS (C₂₇H₂₇Cl₂N₅O₃S [M+H]⁺ m/z 572.1

The absolute stereochemical configuration of JD5037 was determined by x-ray diffraction. JD5037 was dissolved in small amount of isopropanol and then methylene chloride was added. The solution was kept at room temperature overnight to give small crystals. After two days at room temperature larger crystals were obtained. Single-crystal X-ray diffraction data on JD5037 was collected using CuK α radiation and a Bruker Platinum 135 CCD area detector. A 0.023 x 0.079 x 0.129 mm³ crystal was prepared for data collection by coating with high viscosity microscope oil. The oil-coated crystal was mounted on a micro-mesh mount (Mitegen, Inc.) and transferred to the diffractometer and data collected at room temperature. The crystal was monoclinic in space group *C* 2, with unit cell dimensions $a = 19.9407(7)$, $b = 5.4435(2)$, $c = 25.1138(9)$ Å, and $\beta = 90.523(2)^\circ$. Data was 95.5% complete to 68.33° 2θ (approximately 0.83 Å) with an average redundancy of 2.80. The final anisotropic full matrix least-squares refinement on F^2 with 345 variables converged at $R1 = 4.91\%$, for the observed data and $wR2 = 15.32\%$ for all data. The structure was solved by direct methods and refined by full-matrix least squares on F^2 values using the programs found in the SHELXTL suite (Bruker, SHELXTL v6.10, 2000, Bruker AXS Inc., Madison, WI). Corrections were applied for Lorentz, polarization, and absorption effects. Parameters refined included atomic coordinates and anisotropic thermal parameters for all non-hydrogen atoms. Hydrogen atoms on carbons were

included using a riding model [coordinate shifts of C applied to H atoms] with C-H distance set at 0.96 Å.

Mice

Animal protocols were approved by the Institutional Animal Care and Use Committee of the NIAAA, NIH. Male 6-week old C57Bl/6J mice and adult, male, genetically obese *ob/ob* and *db/db* mice with their lean controls were obtained from Jackson Laboratory. Mice were maintained under a 12-h light/dark cycle and fed *ad libitum*. To generate diet-induced obesity (body weight > 42g), C57Bl/6J mice were fed either a high-fat diet (HFD) (Research Diet, D12492; 60% of calories from fat, 20% from protein and 20% from carbohydrates) or a standard laboratory diet (STD, NIH-31 rodent diet) for 12-14 weeks. CB₁^{-/-} mice and their wild-type littermates were generated and backcrossed to a C57Bl/6J background as described (Tam et al., 2010)

Experimental protocol

HFD-fed obese mice received vehicle, JD5037 or SLV319 daily for 7-28 days by oral gavage of 3 mg/kg, as indicated. Age-matched control mice on STD received vehicle daily. Body weight and food intake were monitored daily. Mice were sacrificed by cervical dislocation, the brain, liver, kidney and combined fat pads were removed, weighed, and snap-frozen, and trunk blood was collected for determining endocrine and biochemical parameters. Adiposity index was defined as the combined weight of the epididymal, retroperitoneal and inguinal fat pads, expressed as % of total body weight. Total body fat content and lean mass were determined by EchoMRI-100 (Echo Medical Systems LLC, Houston TX). Adult, male, genetically obese *ob/ob* and *db/db* mice were treated with JD5037 or vehicle for 7 days, and hormonal and metabolic parameters were determined as in mice with DIO.

Tissue levels of antagonists

For acute treatment, mice received a single oral dose (3 mg/kg) of JD5037 or SLV319 and were sacrificed 1 hour later. Blood was collected, and the mice were perfused with phosphate buffered saline for 1 min to remove drug from the intravascular space before removing the brain and liver. For chronic treatment, mice received daily oral doses of 3 mg/kg of either antagonist for 28 days

and were sacrificed 1 hour following the last dose. Tissues and plasma were extracted as described (Mukhopadhyay et al., 2011) and drug levels were determined by liquid chromatography/tandem mass spectrometry (LC-MS/MS) using an Agilent 6410 triple quadrupole mass spectrometer (Agilent Technologies) coupled with an Agilent 1200 LC system (Agilent Technologies). Chromatographic and mass spectrometer conditions were set as described (Godlewski et al., 2010). Levels of each compound were analyzed by multiple reactions monitoring (MRM). The molecular ion and fragments for each compound were measured as follows: m/z 487.2→257.1 and 487.2→193.1 for SLV319 (CID-energy: 20 V and 56 V, respectively), m/z 572.2→555.1 and 572.2→111.0 for JD5037 (CID-energy: 16 V and 72 V, respectively). The acquisition and quantitation of analytes were achieved using MassHunter Workstation LC/QQQ Acquisition and MassHunter Workstation Quantitative Analysis softwares, respectively (Agilent Technologies). The amounts of SLV319 and JD5037 in the samples were determined against standard curves. Values are expressed as ng/g or ng/ml in wet tissue weight or plasma volume, respectively.

Radioligand binding assays

JD5037 and SLV319 binding to CB₁R was assessed in competition displacement assays using [³H]CP-55,940 as the radioligand and crude membranes from mouse brain (Tam et al., 2010). All data were in triplicates with *K_i* values determined from three independent experiments.

[³⁵S]GTPγS binding

Mouse brains were dissected and P2 membranes prepared (Griffin et al., 1998) and resuspended at ~6 μg protein/μl in 1 ml assay buffer (50 mM Tris HCl, 9 mM MgCl₂, 0.2 mM EGTA, 150 mM NaCl; pH 7.4). Ligand-stimulated [³⁵S]GTPγS binding was assayed as described (Tam et al., 2010).

Nonspecific Brain Binding

Non-specific binding of JD5037 to brain was determined by equilibrium dialysis as described (Maurer et al., 2005) using crude brain membrane preparations from CB₁^{-/-} mice incubated with 2 μM JD5037. The bound and unbound levels of JD5037 were determined by LC-MS/MS.

Positron emission tomography (PET)

CNS CB₁R occupancy by JD5037 or SLV319 was also assessed *in vivo* by their ability to displace a CB₁R PET ligand. ¹⁸F-FMPEP-*d2* was synthesized as described (Donohue et al., 2008). The specific activity at the time of injection was 3119 ± 1156 mCi/μmol (mean±SD). The radiochemical purity was greater than 99%. A total of 7 PET experiments in 42 male mice were performed. The mice were fed with either STD or HFD (for 14 weeks) and treated orally with JD5037, SLV319 (3 mg/kg) or vehicle 1 h prior to radioligand injection unless a displacement study was performed in which the drugs were given intravenously 30 min after radioligand injection as indicated in the figure legend. Concurrent to injection of 128 ± 124 μCi of ¹⁸F-FMPEP-*d2*, PET scans began and continued for 120 min on a Siemens microPET Focus 120 camera (Siemens Medical Solutions, Knoxville, TN). Images were reconstructed without attenuation and scatter correction. For each animal, brain time activity curve was constructed and expressed in standardized uptake value which compensates for the injected activity and body weight. Whole brain uptake was determined by area under the time activity curve.

Catalepsy test

Catalepsy was assayed using the bar test as described (Tam et al., 2010).

Locomotor activity

Locomotor activity was quantified by the number of disruptions of infrared beams in two dimensions in an activity chamber.

Elevated plus-maze (EPM) test

Anxiety-related behaviors were assessed using the EPM test as described (Tam et al., 2010).

Upper gastrointestinal transit

Drugs or vehicle were administered orally by gavage 1 h prior to oral administration of the marker (10% charcoal suspension in 5% gum arabic). Thirty min later, mice were killed and the distance travelled by the head of the marker between the pylorus and the caecum was measured and expressed as percent of total length of the small intestine.

Conditioned taste aversion

Male 10-week old C57Bl/6J mice were examined for LiCl or JD5037 induced conditioned taste aversion (CTA) as described previously (Camp et al., 2011), with small modifications. Briefly, singly housed mice were first water-deprived and habituated to drinking from two water-filled sipper tubes offered in the cage for 30 minutes twice per day (9:00 am and 4:00 pm) for 6 days. The following day, mice were offered one tube, containing 0.5% saccharin, at 9:00 am for 30 minutes. Thirty minutes later, mice were given an i.p. injection of 0.15 M LiCl in a volume of 20 ml/kg (= 0.30 M), JD5037 (3 mg/kg) or vehicle and observed for signs of malaise. Mice were offered water during the 4:00 pm presentation to prevent excessive dehydration. CTA was probed 1 day after conditioning where mice were offered two tubes (one containing 0.5% saccharin, the other tap water), for 40 minutes. Evidence of CTA was observed by the preference for one flavor over another, and expressed as the percentage of saccharine consumed/total fluid consumed from both tubes.

Food intake and body weight

The amount of food eaten and body weight were recorded daily. For measuring the effect of leptin on food intake, mice on HFD (14 weeks) were treated orally with JD5037 (3 mg/kg) or vehicle for 7 days. A third group of age-matched controls on STD was treated with vehicle for 7 days. After a week of treatment, mice were treated twice a day with leptin (3 mg/kg, ip.) or vehicle for additional 4 days, and food intake and body weight were measured daily. A separate cohort of DIO mice were treated with daily doses of 5 µg/g of pegylated superactive leptin antagonist (GESLAN) or saline for 5 days. On the third day, half of each group was treated with JD5037 (3 mg/kg) or vehicle, and food intake and body weight was monitored daily.

To test the role of CB₁R blockade in the reversal of hyperleptinemia by JD5037, we measured plasma leptin levels and body weight in DIO mice pair-fed to the daily food intake of JD5037-treated DIO mice.

For measuring the hypophagic effect of an acute oral dose (3 mg/kg) of SLV319, JD5037 or vehicle on food intake in a fasting/refeeding paradigm, lean control or *ob/ob* mice were fasted for 24 h. Half an hour before the onset of the dark period, the mice were treated with the drugs and food was introduced to them 30 min later. Cumulative food intake was then measured hourly for 3 hours.

Blood and urine chemistry

Blood was collected at the time the mice were sacrificed. Serum ALT, AST, HDL- and LDL-cholesterol and triglycerides were quantified using AMS Vegasys Chemistry Analyzer (Diamond Diagnostics). Blood glucose was determined using the Elite glucometer (Bayer). Serum insulin was determined using the Ultra Sensitive Mouse Insulin ELISA kit (Crystal Chem Inc). Serum leptin and adiponectin were determined by ELISA (B-Bridge International). Serum creatinine was determined using QuantiChrom™ Creatinine Assay Kit (BioAssay Systems, CA).

For measurement of leptin in urine, mice on HFD (14 weeks) were treated orally with JD5037 (3 mg/kg) or vehicle for 7 days. A third group of age-matched controls on STD was treated with vehicle for 7 days. After a week of treatment, mice were put in metabolic cages and urine was collected for 24 h, then leptin was determined by ELISA (RayBiotech).

Hepatic triglyceride (TG) content

Liver tissue was extracted as described previously (Folch et al., 1957) and its triglyceride content determined using EnzyChrom™ Triglyceride Assay Kit (BioAssay Systems).

Glucose tolerance (ipGTT) and insulin sensitivity tests (ipIST)

Mice fasted overnight were injected with glucose (1.5 g/kg ip.), followed by tail blood collection at 0, 15, 30, 45, 60, 90 and 120 minutes. Blood glucose levels were determined using the Elite glucometer (Bayer, Pittsburgh, PA). On the following day, mice were fasted for 6 h before receiving insulin (0.75 U/kg, ip.; Eli Lilly), and blood glucose levels were determined at the same intervals as above.

Leptin sensitivity

Leptin sensitivity of lean and DIO mice and DIO mice treated with JD5037 for 7 or 28 days was assessed in 2 paradigms. 1) To test the effect of CB₁ blockade on STAT3 phosphorylation in the hypothalamus, mice were fasted overnight then treated by either vehicle or leptin (3 mg/kg, ip.). One hour later, mice were euthanized and the hypothalamus was collected, snap-frozen on dry ice and kept at -80°C until further analysis. STAT3 phosphorylation was quantified by Western blotting as described below. 2) Leptin sensitivity was also assessed by the ability of subacute

leptin treatment to reduce food intake and body weight. Following chronic treatment of mice with vehicle or JD5037 as described above, the mice received i.p. injections of 3 mg/kg leptin twice daily for 4 days. Body weight before and after this treatment, as well as cumulative food intake during the treatment period had been measured.

Area Postrema lesioning

To assess the involvement of area postrema (AP) in mediating the anorexigenic action of CB₁ blockade, we thermally ablated the AP in DIO mice. Mice on HFD (14 weeks) were anesthetized with isoflurane then transferred to a surgical platform with an infra-red heat source to maintain the animal's body temperature. A dorsal midline incision was made through the skin from just rostral of the nuchal crest to the mid-cervical region. The underlying muscle layers were separated by blunt dissection and using a surgical stereoscope for magnification, the atlanto-occipital membrane was incised exposing the AP. The AP was cauterized using a custom made unipolar probe with an uninsulated area of 0.5 X 0.75 mm, attached to an electrosurgical unit (ACME model 222, set at 1.5 micro-current, for 2 intervals of 2.6 seconds. Then, the muscle layers were sutured and the skin was closed using stainless steel wound clips. Following standard postoperative care, the animals were returned to their home cage for an additional 14 days of high-fat diet and daily monitoring of body weight.

The AP ablation was functionally tested by verifying the effect of an acute dose (5 µg/kg) of amylin on food intake. Briefly, AP-ablated (APX) and control mice were fasted for 24 h, then injected with either amylin (Phoenix Pharmaceuticals, Inc.) or saline intraperitoneally and food intake was measured for 2 h after injection. Recovered from this test, the mice were orally treated with either JD5037 (3 mg/kg) or vehicle for 7 days and food intake and body weight were monitored daily. Leptin sensitivity test was performed as described above. After completion of all the feeding experiments, APX and control mice were sacrificed, the brain removed and 5 µm-thick, paraffin-mounted coronal sections of the AP region prepared for histological analysis.

Indirect calorimetry and locomotor activity

O₂ consumption and CO₂ production were monitored by indirect calorimetry (Oxymax, Columbus Instruments) with one mouse per chamber as described (Tam et al., 2010).

Western blotting

STAT3, SOCS3, megalin and RAP relative tissue contents were assessed by Western blotting (Liu et al., 2000) using an antibody specific for STAT3 phosphorylated on ty_{R705}, a second antibody that detected total STAT3 (Cell Signaling), and antibodies specific for SOCS3 (Cell Signaling), megalin and RAP (Abcam).

The cellular levels of human megalin in RPTEC were determined by Western blotting using antibodies specific for megalin (Proteintech, IL).

Immunoprecipitation

Active G_{iα} was immunoprecipitated using Pierce Classic IP Kit according to the manufacturer's protocol. Briefly, 3T3-L1 adipocytes were cultured in 6-well plates until day 14 of differentiation. Before the treatment, cells were incubated for 24 h in a serum-free adipocyte maintenance medium (ZenBio, Cat# AM-1-L1-SF), then treated with HU-210 (100 nM), noladin ether (100 nM), AEA (500 nM), AM-3506 (100 nM), JD5037 (100 nM), pertussis toxin (100 ng/ml) or vehicle (0.5% DMSO) for 1 h. Cells were harvested, lysed and 100 µg protein lysate from each sample was incubated overnight with an active G_{iα} mouse monoclonal antibody (Neweast Biosciences) at 4°C. The antibody-lysate complex was captured on Protein A/G plus Agarose in a spin column, washed and eluted in 50 µl of non-reducing Lane Marker Sample Buffer and 20 mM DTT and incubated for 10 min at 100 °C. Samples were loaded onto a Bio-Rad Criterion gel, and Western blotting was performed using the anti-G_{iα} monoclonal antibody (Neweast Biosciences).

Real-time PCR

Total mRNA from mouse epididymal adipose tissue, choroid plexus or kidney was extracted using RNeasy kit (QIAGEN) followed by DNase I treatment (Invitrogen), and reverse-transcribed using the Iscript cDNA kit (Bio-Rad). Real-time PCR was performed using a Bio-Rad iCycler iQ and the QuantiTect Primer Assays (QT00164360, QT01756160 and QT01062691) against mouse leptin, β₃ adrenergic receptor and megalin, respectively. Normalization was performed with the QuantiTect Primer Assay against mouse GAPDH (QT01658692).

Total mRNA from human renal proximal tubule epithelial cells (RPTEC) were extracted as above and Real-time PCR was performed using the QuantiTect Primer Assays (QT00017451, QT00071750, QT02305702 and QT00086583) against human megalin, PPAR α , CB₁ receptor and RAP, respectively. Normalization was performed with the QuantiTect Primer Assay against human β -actin (QT01680476).

Cell culture

3T3-L1 cells were obtained from ZenBio (Research Triangle Park, NC) and cultured at 37°C in a humidified atmosphere of 5% CO₂/95% air. The cells were maintained in a preadipocyte medium (ZenBio, Cat# PM-1-L1). Differentiation of the cells was initiated 48 h after confluence by incubation for 3 days in culture differentiation medium with insulin, dexamethasone and a PPAR γ agonist (ZenBio, Cat# DM-2-L1). This was followed by maintenance in adipocyte feeding medium renewed every 2-3 days (ZenBio, Cat# AM-1-L1). All experiments were conducted using differentiated cells (~80-95%) on day 14 and 15 of differentiation.

RPTEC were obtained from Lonza (Walkersville, MD) and cultured at 37°C in a humidified atmosphere of 5% CO₂/95% air. The cells were maintained in the renal epithelial basal medium containing 10 μ g/ml recombinant human epidermal growth factor, 5 μ g/ml insulin, 0.5 mg/ml hydrocortisone, 0.5% FBS, 0.5 μ g/ml epinephrine, 6.5 μ g/ml T3, 10 mg/ml transferrin, 10 mg/ml gentamicin and 50 μ g/ml amphotericin-B. Cells were used between passages 3 and 9 at >80% confluence.

Leptin secretion assay

Leptin secretion from adipocytes *in vitro* was quantified as described (Zeigerer et al., 2008), with modifications. Briefly, 3T3-L1 adipocytes were cultured in 6-well plates until day 14 of differentiation. Before any treatment, cells were incubated for 24 h in a serum-free adipocyte maintenance medium (ZenBio, Cat# AM-1-L1-SF). Leptin secretion was measured in the presence of HU-210 (100 nM), nolidin ether (100 nM), AEA (500 nM), AM-3506 (100 nM), WIN 55,212-2 (1 μ M), JD5037 (100 nM) or vehicle (0.5% DMSO) for an additional 24 h in the presence or absence of pertussis toxin (PTX) at 100 ng/ml. At the end of the incubation period, the medium was collected and frozen at -80°C for subsequent determination of leptin concentration. Three wells of 6-well plate were collected per treatment in three independent

experiments. Medium samples were concentrated using an YM-10 centrifugal filter (Millipore) and assayed for leptin levels using a mouse leptin ELISA kit (RayBiotech). The amount of leptin released into the medium at each time point was normalized to total protein content using Bradford procedure. Leptin values were expressed as pg/ml/mg protein.

Adipose tissue norepinephrine levels

Norepinephrine (NE) was determined in the epididymal fat pad using a modification of a previously published method (Tam et al., 2008). In short, following separation, the epididymal fat pads were weighed and homogenized in (100 μ l/10 mg tissue) extraction buffer containing 0.1M perchloric acid and 20 ng 3,4-dihydroxybenzylamine (DHBA) as an internal standard. The homogenates were centrifuged and the supernatant was transferred to 10 mM Na₂S₂O₅ solution containing acid-washed alumina with subsequent addition of 1 ml of 1 M Trizma Base containing 2% EDTA. The samples were vortexed and centrifuged and the supernatant was discarded. The alumina was then washed with water and the NE desorbed from the alumina with 0.1 M perchloric acid. NE was quantified by high performance liquid chromatography with electrochemical detection, using a 15 cm ion-pair chromatography column (Luna 5 μ C18; Phenomenex). The column was eluted with a mobile phase containing 2.8 g 1-heptanesulfonic acid sodium salt, 0.17 g EDTA, 20 ml triethylamine, dissolved in 2.2 L H₂O, pH adjusted to 2.5 with 13 ml 85% phosphoric acid, plus 90 ml acetonitrile. The flow rate was 0.4 ml/min with electrochemical detector sensitivity at 50 nA and applied potential of 0.7 V. Measurements were made using the internal DHBA standard as reference.

Leptin clearance

Recombinant human leptin (R & D Systems) was injected i.p. at a dose of 10 mg/kg to mice fed STD or HFD for 14 weeks, or to HFD-fed mice treated with JD5037 (3 mg/kg p.o.) for 7 days. Blood samples were taken from the mandibular vein at 60, 180, 300, 360, 420 and 480 min. Serum was immediately separated and human leptin level was determined by ELISA (Millipore Corporation). Terminal elimination rate constant was determined by linear regression of the last 3 measurable concentrations and the terminal half-life of leptin calculated as described (Wong et al., 2004).

Chronic infusion of leptin

To assess the effects of hyperleptinemia on the response to peripheral CB₁ antagonism in DIO mice, vehicle (saline), mouse leptin (R & D; 1 or 3 mg/kg/day) or human leptin (R & D; 3 mg/kg/day) was delivered over 7 days by subcutaneous infusion, using osmotic minipumps (model 2001D, Alzet Osmotic Pumps; Durect, Cupertino, CA) and the effect of simultaneous 7-day treatment with daily oral doses of vehicle or JD5037 (3 mg/kg) on body weight, food intake, serum leptin levels and STAT3 phosphorylation in the hypothalamus were determined as described above.

Measurement of ¹²⁵I-leptin internalization and degradation

RPTEC were seeded (2×10^5 cells/well) and grown to 80-90% confluence as described above in 6-well plates at 37°C in a humidified atmosphere of 5% CO₂/95% air. Medium was replaced every other day and cells were treated with vehicle, JD5037 (1 μM) or HU-210 (100 nM) 24 h before the experiment. To study ¹²⁵I-leptin internalization, medium was aspirated and the cells were incubated in fresh complete regular medium with 10 nM cold human leptin (R & D Systems, MN) in the presence of 30,000 cpm ¹²⁵I-leptin for 20 min to allow internalization but not degradation. Cells were then placed on ice, the medium was removed, and intracellular ¹²⁵I-leptin was determined by measuring the cell-associated radioactivity by γ counter after solubilization in 1 ml of 1 M NaOH and was calculated as percentage of total ¹²⁵I-leptin activity in the vehicle group.

For degradation assays, the cells were treated as above but incubated for 2 h. After incubation, the culture media were collected and precipitated with 20% trichloroacetic acid (TCA), and the radioactivity of the TCA-soluble degradation products was quantified by γ counter. To correct for liberation of iodine from ¹²⁵I-leptin during the experiment, medium was incubated in a well without cells. The amount of the TCA-soluble radioactive fraction found in the medium was then subtracted from the TCA-soluble radioactive fraction found in the samples.

Collecting cerebrospinal fluid (CSF) from mice

CFS samples were withdrawn from the cisterna magna as described (Liu and Duff, 2008), with modifications. Briefly, animals were anesthetized intraperitoneally with ketamin (100 mg/kg) and xylazine (10 mg/kg) and kept on heating pads. The skin of the neck was shaved and the

mouse was placed prone on a stereotaxic instrument and a sagittal incision of the skin was made inferior to the occiput. Under a dissection microscope, the subcutaneous tissue and muscles were separated and the mouse was laid down so that the head forms a nearly 135° angle with the body. The dura mater was blotted dry with sterile cotton swab and a glass capillary tube was penetrated into the cisterna magna through the dura mater. CSF (~7-10 µl) taken up by the capillary tube and was transferred into an Eppendorf tube and frozen immediately on dry ice. Leptin levels in CSF were assayed using a mouse leptin ELISA kit (RayBiotech).

Endocannabinoid measurements by LC/MS/MS.

RPTEC (1×10^5 cells) were seeded in 10 cm² dishes and grown to 90% confluency. 24 h before extraction, the medium was removed and replaced by fresh medium with or without FBS. After an additional 24 h, the medium was removed and cells were washed twice in 1xPBS, harvested and collected into 5 ml tubes. The cells were sonicated in 200 µl PBS and further extraction and measurement of anandamide and 2-AG was performed as described previously (Mukhopadhyay et al., 2011). Values are expressed as total ng/dish.

Epididymal fat-pad denervation.

DIO mice were anesthetized with isoflurane, the epididymal fat pads (EPI) were exposed and a series of 20 microinjections (2 µl per injection) of either saline or 10 mg/ml 6-OHDA dissolved in 0.01 M PBS, 1% ascorbic acid was made evenly throughout the pad using a 10 µl Hamilton syringe. The needle was held in place for ~30 s after each injection to minimize backflow. Following the injections, the fat pads were irrigated with saline, repositioned and the abdominal cavity was closed with absorbable sutures in two layers. Animals were allowed to recover from the surgery for 2 weeks and then treated for 7 days with JD5037 (3 mg/kg, po) or vehicle. The animals were then euthanized and the EPI pads were collected and snap-frozen in dry ice for measurement of NE content.

Materials

Rimonabant and CP-55,940 was obtained from the National Institute of Drug Abuse Drug Supply Program. HU-210, noladin ether, anandamide and WIN55,212-2 were purchased from Tocris. GESLAN was purchased from Protein Laboratories Rehovot (PLR) Ltd, Israel.

SUPPLEMENTAL REFERENCES

- Camp, M.C., Feyder, M., Ihne, J., Palachick, B., Hurd, B., Karlsson, R.M., Noronha, B., Chen, Y.C., Coba, M.P., Grant, S.G., *et al.* (2011). A novel role for PSD-95 in mediating ethanol intoxication, drinking and place preference. *Addict Biol* *16*, 428-439.
- Donohue, S.R., Krushinski, J.H., Pike, V.W., Chernet, E., Phebus, L., Chesterfield, A.K., Felder, C.C., Halldin, C., and Schaus, J.M. (2008). Synthesis, ex vivo evaluation, and radiolabeling of potent 1,5-diphenylpyrrolidin-2-one cannabinoid subtype-1 receptor ligands as candidates for in vivo imaging. *J Med Chem* *51*, 5833-5842.
- Folch, J., Lees, M., and Sloane Stanley, G.H. (1957). A simple method for the isolation and purification of total lipides from animal tissues. *J Biol Chem* *226*, 497-509.
- Godlewski, G., Alapafuja, S.O., Batkai, S., Nikas, S.P., Cinar, R., Offertaler, L., Osei-Hyiaman, D., Liu, J., Mukhopadhyay, B., Harvey-White, J., *et al.* (2010). Inhibitor of fatty acid amide hydrolase normalizes cardiovascular function in hypertension without adverse metabolic effects. *Chem Biol* *17*, 1256-1266.
- Griffin, G., Atkinson, P.J., Showalter, V.M., Martin, B.R., and Abood, M.E. (1998). Evaluation of cannabinoid receptor agonists and antagonists using the guanosine-5'-O-(3-[35S]thio)-triphosphate binding assay in rat cerebellar membranes. *J Pharmacol Exp Ther* *285*, 553-560.
- Lange, J.H., Coolen, H.K., van Stuivenberg, H.H., Dijksman, J.A., Herremans, A.H., Ronken, E., Keizer, H.G., Tipker, K., McCreary, A.C., Veerman, W., *et al.* (2004). Synthesis, biological properties, and molecular modeling investigations of novel 3,4-diarylpyrazolines as potent and selective CB(1) cannabinoid receptor antagonists. *J Med Chem* *47*, 627-643.
- Liu, J., Gao, B., Mirshahi, F., Sanyal, A.J., Khanolkar, A.D., Makriyannis, A., and Kunos, G. (2000). Functional CB1 cannabinoid receptors in human vascular endothelial cells. *Biochem J* *346 Pt 3*, 835-840.
- Liu, L., and Duff, K. (2008). A technique for serial collection of cerebrospinal fluid from the cisterna magna in mouse. *J Vis Exp*.
- Maurer, T.S., Debartolo, D.B., Tess, D.A., and Scott, D.O. (2005). Relationship between exposure and nonspecific binding of thirty-three central nervous system drugs in mice. *Drug Metab Dispos* *33*, 175-181.
- Mukhopadhyay, B., Cinar, R., Yin, S., Liu, J., Tam, J., Godlewski, G., Harvey-White, J., Mordi, I., Cravatt, B.F., Lotersztajn, S., *et al.* (2011). Hyperactivation of anandamide synthesis and regulation of cell-cycle progression via cannabinoid type 1 (CB1) receptors in the regenerating liver. *Proc Natl Acad Sci U S A*.
- Tam, J., Trembovler, V., Di Marzo, V., Petrosino, S., Leo, G., Alexandrovich, A., Regev, E., Casap, N., Shteyer, A., Ledent, C., *et al.* (2008). The cannabinoid CB1 receptor regulates bone formation by modulating adrenergic signaling. *FASEB J* *22*, 285-294.
- Tam, J., Vemuri, V.K., Liu, J., Batkai, S., Mukhopadhyay, B., Godlewski, G., Osei-Hyiaman, D., Ohnuma, S., Ambudkar, S.V., Pickel, J., *et al.* (2010). Peripheral CB1 cannabinoid receptor blockade improves cardiometabolic risk in mouse models of obesity. *J Clin Invest* *120*, 2953-2966.

Wong, S.L., DePaoli, A.M., Lee, J.H., and Mantzoros, C.S. (2004). Leptin hormonal kinetics in the fed state: effects of adiposity, age, and gender on endogenous leptin production and clearance rates. *J Clin Endocrinol Metab* 89, 2672-2677.

Zeigerer, A., Rodeheffer, M.S., McGraw, T.E., and Friedman, J.M. (2008). Insulin regulates leptin secretion from 3T3-L1 adipocytes by a PI 3 kinase independent mechanism. *Exp Cell Res* 314, 2249-2256.